Direct evidence of lipid translocation between adipocytes and prostate cancer cells with imaging FTIR microspectroscopy

Ehsan Gazi,[1,*] Peter Gardner,[†] Nicholas P. Lockyer,[†] Claire A. Hart,[*] Michael D. Brown,[*] and Noel W. Clarke[*,§,]**

ProMPT Genito Urinary Cancer Research Group, Paterson Institute for Cancer Research,* and School of Chemical Engineering and Analytical Science,† The University of Manchester, Manchester, UK; Department of Urology, Hope Hospital,§ and Department of Urology, Christie Hospital,** NHS Trust, Manchester, UK

Abstract **Various epidemiological studies show a positive correlation between high intake of dietary FAs and metastatic prostate cancer (CaP). Moreover, CaP metastasizes to the bone marrow, which harbors a rich source of lipids stored within adipocytes. Here, we use Fourier transform infrared (FTIR) microspectroscopy to study adipocyte biochemistry and to demonstrate that PC-3 cells uptake isotopically labeled FA [deuterated palmitic acid (D_{31}-PA)] from an adipocyte. Using this vibrational spectroscopic technique, we detected subcellular locations in a single adipocyte enriched with D_{31}-PA using the $\upsilon_{as+s}(C\text{-}D)_{2+3}$ (D_{31}-PA): $\upsilon_{as+s}(C\text{-}H)_{2+3}$ (lipid hydrocarbon) signal. In addition, larger adipocytes were found to consist of a higher percentage of D_{31}-PA of the total lipid found within the adipocyte. Following background subtraction, the $\upsilon_{as}(C\text{-}D)_{2+3}$ signal illuminated starved PC-3 cells cocultured with D_{31}-PA-loaded adipocytes, indicating translocation of the labeled FA. This study demonstrates lipid-specific translocation between adipocytes and tumor cells and the use of FTIR microspectroscopy to characterize various biomolecular features of a single adipocyte without the requirement for cell isolation and lipid extraction.**—Gazi, E., P. Gardner, N. P. Lockyer, C. A. Hart, M. D. Brown, and N. W. Clarke. **Direct evidence of lipid translocation between adipocytes and prostate cancer cells with imaging FTIR microspectroscopy.** ***J. Lipid Res.*** **2007.** 48: **1846–1856.**

Supplementary key words tumor • fatty acids • Fourier transform infrared spectroscopy • deuterated palmitic acid

In the United Kingdom, prostate cancer (CaP) is the most commonly diagnosed cancer in men (1) and the second most common cause of cancer-related death in men (2). Several epidemiological studies have shown that total dietary intake of FAs, as well as specfic FAs, potentiate an increased risk of CaP (3–5). Dennis et al. (5) conducted a detailed review of 29 epidemiological studies investigating this relationship and identified associations of advanced CaP with intake of total and saturated fat, using pooled relative risks of five studies for each comparison (5). This association is also shown in several reports demonstrating that prostate tumors of obese men exhibit clinical features that are characteristic of accelerated progression (6, 7).

The linkage between lipids and advanced CaP may also be reflected in the natural history of this disease, because it is well documented that circulating metastatic CaP cells in the peripheral blood possess a predilection for deposition into the bone marrow stroma (BMS) (8), which harbors a rich source of lipids stored within adipocytes. Brown et al. (9) have shown that PC-3 cell (human CaP cell line derived from bone metastases) invasion toward BMS was significantly reduced when the experiment was repeated with BMS grown in the absence of hydrocortisone so that adipocyte formation was not stimulated.

Adipocytes are specialized for the synthesis and storage of FAs as triacylglycerides (TAGs) (10) and for FA mobilization through lipolysis (11) in response to hormones, cytokines, and other factors involved in energy metabolism (12). In recent years, there has been growing interest in understanding the interactions of CaP cells with adipocytes at the molecular level (9, 13, 14). Tokuda et al. (13) have shown that adipocytes cocultured with PC-3 cells influenced not only the differentiation growth patterns of the PC-3 cells but also their proliferative rate. Oil Red O staining for neutral lipids and transmission electron microscopy revealed larger and greater frequency of lipid droplets within the cytoplasm of cocultured PC-3 cells

Manuscript received 19 March 2007 and in revised form 24 April 2007.

Published, JLR Papers in Press, May 11, 2007.
DOI 10.1194/jlr.M700131-JLR200

Abbreviations: BMS, bone marrow stroma; CaP, prostate cancer; CPD, critical-point drying; D_{31}-PA, deuterated palmitic acid; FFA, free FA; FTIR, Fourier transform infrared; IL-6, interleukin-6; IR, infrared; MSC, mesenchymal stem cell; PF, paraformaldehyde; SR, synchrotron; TAG, triacylglyceride.

[1] To whom correspondence should be addressed.
e-mail: EGazi@picr.man.ac.uk

compared with the control (PC-3 monoculture) (13). Previously, we have demonstrated through Fourier transform infrared (FTIR) microspectroscopic imaging that metastatic CaP cells in bone marrow tissue, with close proximity to adipocytes, give rise to higher lipid hydrocarbon signals relative to distant CaP cells (9). FTIR microspectroscopy is an optically based technique that can measure the transitions in vibrational modes (mainly stretching and bending) of the functional groups of biomolecular constituents within cells, as a result of absorption and subsequent excitation by infrared (IR) radiation. The functional group vibrations are representative of biomolecular constituents such as lipids, proteins, carbohydrates, and a variety of phosphorylated molecules. The FTIR spectrum derived from the cell comprises a series of peaks as a function of wave number, which depict the state of chemical bonding (intra- and intermolecular hydrogen bonding, van der Waals interactions, and steric factors) and the relative intensities of the above-mentioned species within the scrutinized area of the cell.

Although CaP cells in the presence of adipocytes exhibit higher lipid signals (9, 13), there have been no data in the literature that unequivocally establishes whether this increase is the result of adipocyte-to-CaP cell lipid transposition or is due to adipocyte-secreted cytokine stimulation of CaP cells, such as with interleukin-6 (IL-6) (14, 15), which may elicit de novo lipid synthesis. IL-6 has been reported to augment de novo lipid synthesis of FAs in hepatocytes of mice (16). Furthermore, accepting that lipid molecules are transferred from adipocytes into CaP cells, it is not known whether this process is selective toward specific FAs that are required by the CaP cell. Here, we use imaging FTIR microspectroscopy as an analytical methodology for *i*) the biomolecular characterization of the adipocyte following loading with deuterated FA and *ii*) studying the translocation of deuterated FA between adipocytes and PC-3 cells, following fixation.

MATERIALS AND METHODS

PC-3 cell-adipocyte cocultures

Human preadipocytes were derived from mesenchymal stem cells (MSCs) isolated from primary human BMS of the rib (obtained with patient consent and under ethical approval) using the RosetteSep procedure (StemCell Technologies), following the manufacturer's guidelines (17). Briefly, bone marrow was mixed and incubated with RosetteSep™ Human MSC Enrichment Cocktail for 20 min at room temperature. This sample was diluted with PBS + 2% FBS and 1 mM EDTA and layered on Ficoll-Paque®. This was centrifuged at 300 *g* for 25 min, and the enriched MSCs were removed and washed with PBS containing 2% FBS and 1 mM EDTA. Following this, the MSCs were cultured to 80% confluency onto 70% (v/v) ethanol-sterilized MirrIR plates in MesenCult® basal medium with antibiotic/antimycotic (Invitrogen) solution at 37°C, 5% CO_2 in air. Induction of adipogenesis was carried out by replacing the MesenCult® basal medium with adipogenic tissue-stimulatory media (MesenCult® basal medium with adipogenic-stimulatory supplements and antibiotic/antimycotic solution) containing 50 μM deuterated palmitic acid (D_{31}-PA) in ethanol (Sigma-Aldrich, UK), with incubation at 37°C, 5% CO_2 for 12 days. The adipogenic tissue-stimulatory medium with 50 μM D_{31}-PA was changed once during this period on day 6. On day 12, differentiated adipocytes were washed twice with PBS, and 8×10^4 serum-starved PC-3 cells precultured in RPMI (Cambrex) with 1% L-glutamine (Sigma-Aldrich) for 24 h were added to the culture. Following this, the cocultures were grown in RPMI with 1% L-glutamine for 48 h.

Cell fixation

Cultures on MirrIR plates were washed twice with PBS and then fixed in 4% paraformaldehyde (PF) in PBS for 25 min. Following this, the cells were washed three times (5 min each wash) in Sorensen's buffer (0.15 M, pH 7.4) to remove free PF. The cells were postfixed in 1% osmium tetroxide (OsO_4) for 1 h and washed a further three times (5 min each wash) with Sorensen's buffer prior to dehydration using increasing concentrations of ethanol-water (30:70, 50:50, 70:30, 90:10) for 5 min. The cells were placed twice in 100% ethanol for 5 min. The cells were then transferred to Arklone (112 trichloro-122 trifluroethane; TAA Laboratories, UK) and placed into the precooled (9°C) chamber of the critical-point drier (Bal-tec CPD-030). The Arklone was substituted for liquid CO_2 following five Arklone-CO_2 exchanges, and then a 5 min immersion (this procedure was repeated twice again). Phase-transition was induced by heating the chamber to 40°C and at 80 bar pressure. Preservation was assessed by a high-power optical microscope. The cells were stored in a desiccator until FTIR analysis. A separate set of adipocytes on MirrIR was fixed in 4% formalin in PBS for 20 min. These cells were then briefly washed in distilled water for 3 s to remove residual PBS from the surface of the cells (17). The cells were dried under ambient conditions and stored in a desiccator until FTIR analysis.

FTIR microspectroscopy

A TAG mix [containing triacetin (C2:0), tributyrin (C4:0), tricaproin (C6:0), tricaprylin (C8:0), and tricaprin (C10:0)] (Sigma-Aldrich) was analyzed in reflection mode by FTIR after smearing a small amount onto an MirrIR slide. The FTIR spectrum was collected using a Nicolet Magna 550 spectrometer, coupled to a Nicplan microscope equipped with a liquid nitrogen-cooled mercury cadmium telluride detector, using a sampling aperture size of 60 μm × 60 μm. The FTIR spectrum represents an average of 512 scans in the wave number range 750–4,000 cm^{-1} with a resolution of 4 cm^{-1}. The sample spectrum was ratioed to a background spectrum that was recorded on a blank area of the plate to correct for the instrument function plus atmospheric CO_2 and water vapor absorptions. FTIR spectra of the subcellular lipid deposit of a formalin-fixed, water-rinsed, and air-dried adipocyte and a PF-OsO_4-CPD-fixed adipocyte were collected at the Daresbury Laboratory (Beamline 11.1) using synchrotron (SR)-based FTIR microspectroscopy. The SR source provides high signal-to-noise spectra with aperture sizes close to the diffraction limit of IR light. For this, a Nicolet Nexus FTIR spectrometer equipped with a liquid nitrogen-cooled mercury cadmium telluride detector and a KBr beam splitter coupled to a Nicolet Continum microscope was used in reflectance mode with a 10 μm × 10 μm sampling aperture. The sample spectrum was collected at 4 cm^{-1} spectral resolution with 128 scans and was ratioed to a background spectrum that was recorded on a blank area of the plate. High-definition FTIR microspectroscopic maps of PF-OsO_4-CPD-fixed adipocyte-PC-3 cell cocultures were collected in reflectance mode at 6.25 μm pixel resolution in rapid-scan mode using a Perkin Elmer Spotlight spectrometer with a 16 × 1 MCT linear array detector. The background scan was recorded at 8 cm^{-1} spectral resolution with 75 scans, whereas the sample scan was recorded at 8 cm^{-1}

spectral resolution with 64 scans. A charged-coupled detector camera, integrated into the Spotlight spectrometer, was used to obtain optical images of the mapping area.

Data analysis

The FTIR spectra of the TAG reference standard and of the lipid deposit of a formalin-fixed, water-rinsed, and air-dried adipocyte were recorded using the OMNIC v.5.1a software, which also included the Atlμs video capturing program. FTIR spectral maps of PF-OsO_4-CPD-fixed adipocyte-PC-3 cell cocultures were processed with Spotlight version 1.0.1. This software permitted the intensity of baseline corrected areas of selected peaks as well as ratio of peaks to be mapped across the map. Adipocyte size in micrometers was determined with ImageJ (version 1.36b) software using optical images captured at ×320 by the charged-coupled detector camera attached to the SR-FTIR Nicolet Nicplan microscope.

RESULTS

Evaluating adipocyte preservation for FTIR microspectroscopy

Figure 1A shows the appearance of adipocytes in growth medium and illustrates the formation of numerous lipid

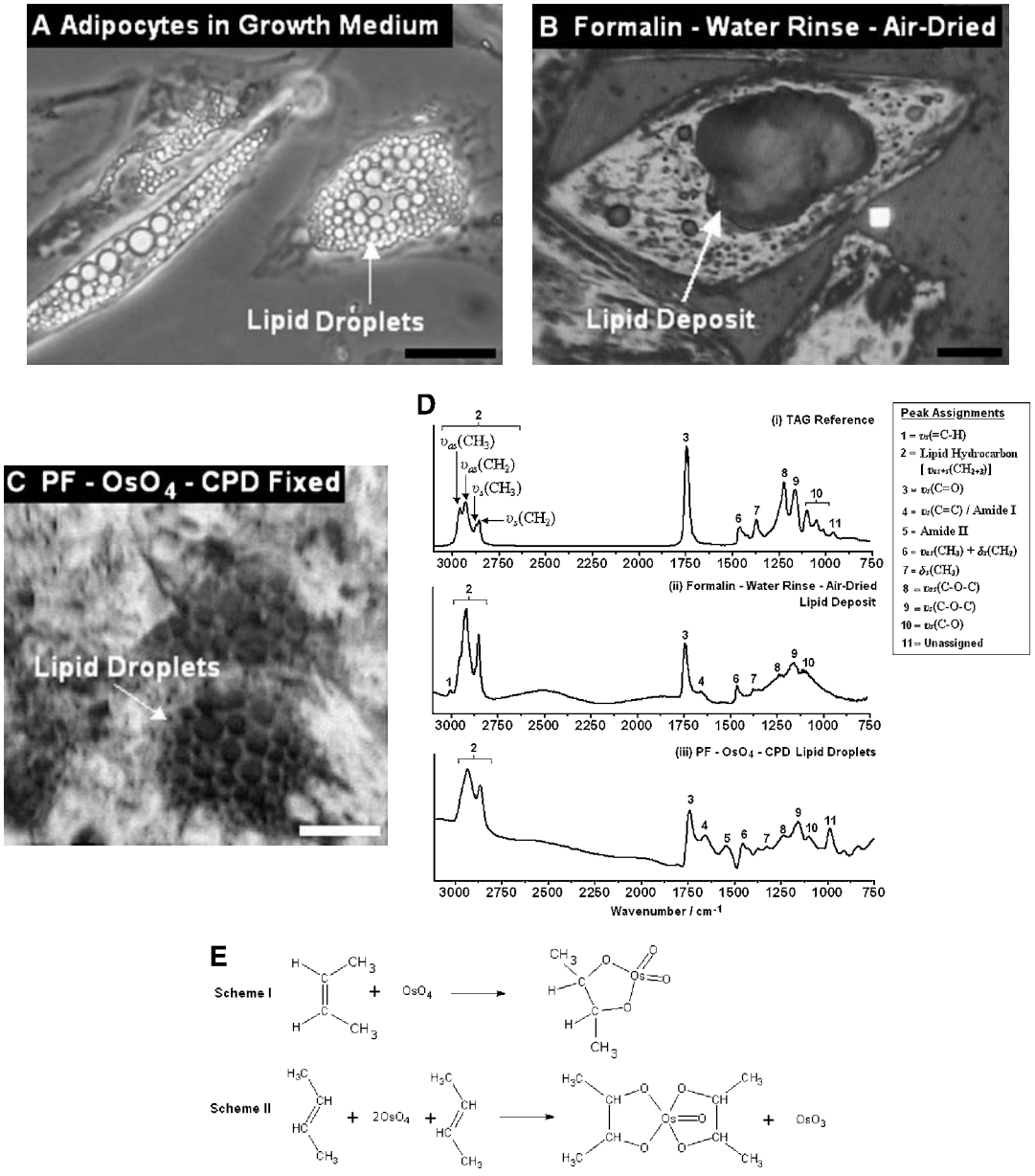

Fig. 1. Adipocyte preparation for FTIR microspectroscopy. Optical photomicrographs showing A: Adipocytes in growth medium with prominent intracellular droplets (scale bar = 10 μm). B: Adipocyte following formalin fixation, water rinsing, and air drying (scale bar = 20 μm). C: Adipocytes fixed in paraformaldehyde (PF) and osmium tetroxide (OsO_4) and critical-point dried (CPD) (scale bar = 30 μm). D: Typical Fourier transform infrared (FTIR) spectrum of (i) triacylglyceride (TAG) reference with C_2 – C_{10}-saturated hydrocarbon chains, (ii) the lipid deposit from a formalin-fixed air-dried adipocyte, and (iii) the lipid droplets from a PF-OsO_4-CPD adipocyte. E: OsO_4 reaction with unsaturated hydrocarbon chains to form cyclic esters. Scheme I: Reaction with a single unsaturated hydrocarbon chain. Scheme II: Cross-linking reaction with adjacent unsaturated hydrocarbon chains.

droplets contained within their cytoplasm. Figure 1B shows adipocytes, prepared for FTIR analysis, following fixation in 4% formalin (in PBS), a brief water rinse to remove residue salts, and air drying at ambient conditions. The water rinse step is of importance in this protocol because salts interfere with FTIR analysis through light scatter, provide low visibility of the sample, and give rise to artifactual phosphate absorption (18). Although we have previously shown that this fixation protocol preserves the localizations of biomolecules in SR-based FTIR images of PC-3 cells (18), in the case of adipocytes, this fixation results in the collapse of intracellular lipid droplet structures into an unordered lipid deposit (Fig. 1B). An FTIR spectrum was extracted from the intracellular lipid deposit of a formalin-fixed, air-dried adipocyte (Fig. 1Dii). This spectrum (Fig. 1Dii) exhibits a lipid ester υ_s(C=O) peak at 1,744 cm^{-1} of the same frequency of absorption as the lipid ester υ_s(C=O) peak in the reference TAG spectrum (Fig. 1Di). Note: the lipid ester υ_s(C=O) peak of glycerol-bound FAs is at higher frequency compared with the lipid υ_s(C=O) peak of free FAs (1,725–1,690 cm^{-1}) (19–21). Several other characteristic peaks of the glycerol moiety of TAG are also observed in the lipid deposit of the formalin-fixed adipocyte at frequencies >1,500 cm^{-1}, and these are identified in Fig. 1Dii as peaks 8–12. However, the peaks in this spectrum (Fig. 1Dii) are broader, compared with the same peaks in the reference TAG spectrum (Fig. 1Di). This is due to the collapse of the lipid droplets, which gives rise to a range of bonding strengths with neighboring molecular species for those functional groups absorbing at frequencies >1,500 cm^{-1}.

Figure 1C shows adipocytes containing well-preserved lipid droplets following PF fixation with OsO_4 postfixation and critical-point drying (CPD). There are several advantages to this sample preparation over formalin fixation, water rinsing, and air drying: *a*) Formalin in PBS contains methanol, which permeates the plasma membrane and results in a faster fixation rate compared with PF, which does not contain methanol. However, methanol extracts intracellular lipids, which is inappropriate for adipocyte fixation. *b*) The OsO_4 postfixative preserves lipids; however it does not absorb in the mid-IR range. *c*) The three-dimensional structure of the adipocyte is retained because the sample is dried without surface tension effects, through CPD, and the localization of the intracellular lipid droplets of the adipocyte is preserved. However, the disadvantage of this fixation protocol is that the mode of action by which OsO_4 preserves lipids is through complexation reaction within the double bonds of lipid hydrocarbon chains or complexation and cross-linking between unsaturated hydrocarbon chains (Fig. 1E). Thus, the υ_s(=C-H) signal from unsaturated hydrocarbons is present in the lipid deposit spectrum of the formalin-fixed, water-rinsed, air-dried adipocyte (Fig. 1Dii), but is not observed in the lipid droplet spectrum of the PF-OsO_4-CPD adipocyte (Fig. 1Diii). Additionally, both methods of fixation (formalin-fixed, water-rinsed, air-dried and PF-OsO_4-CPD) result in a decrease in peak resolution of the $\upsilon_{as}(CH)_2$ and $\upsilon_{as}(CH)_3$ modes, which is also the case for the $\upsilon_s(CH)_2$ and $\upsilon_s(CH)_3$ modes.

FTIR biomolecular characterization of adipocytes

Figure 2Ai shows an optical photomicrograph of a cluster of adipocytes, loaded with isotopically labeled palmitic acid (D_{31}-PA), following PF-OsO_4-CPD fixation. The dark features within this optical image represent the lipid droplets retained within the fully differentiated adipocytes. A negative image (Fig. 2Aii) of Fig. 2Ai provides better visualization of these lipid droplets within the adipocytes. These adipocytes are surrounded by a potentially heterogeneous population of stroma cells. Typical raw FTIR spectra extracted from a fully differentiated adipocyte and from a stroma cell location [points 1 and 2, respectively, in the optical photomicrograph (Fig. 2A)] are shown in Fig. 2B. The incorporation of D_{31}-PA into the adipocyte lipid droplets is confirmed by the presence of the C-D peaks that are clearly observed within the spectral region 2,250–2,000 cm^{-1} (Fig. 2B). This spectral region does not overlap with IR absorbencies from endogenous FAs or other endogenous biomolecular functional group vibrations arising from the adipocyte, as seen in the adipocyte spectrum incubated with no D_{31}-PA (Fig. 1Diii).

The stroma cell spectrum is a typical epithelial cell spectrum, exhibiting a high protein amide I signal relative to other biomolecular constituents, whereas the fully differentiated adipocyte spectrum closely resembles the spectrum of TAG (Fig. 1Di), with an intense lipid υ_s(C=O) peak, glycerol and lipid hydrocarbon signals, and relatively lower amide I and II signals. The area shown in Fig. 2A was analyzed with imaging FTIR microspectroscopy, and the resulting FTIR peak extracted images are shown in Fig. 2C–F. The method of baseline integration (blue line) and peak areas (in gray) used to generate the images in Fig. 2C–F are shown in Fig. 2B.

Figure 2C shows the lipid hydrocarbon:amide I peak area intensity distribution across this imaging field. As expected, the lipid hydrocarbon signal intensity (Fig. 2C) is greatest in the lipid droplets contained within the adipocytes and is lower in the stroma cells. This signal distribution is also reflected by the lipid ester υ_s(C=O) intensity map shown in Fig. 2D, which provides better contrast between adipocytes and stroma cells, compared with the lipid hydrocarbon signal. The intensity distribution of the $\upsilon_{as}(C\text{-}D)_{2+3}$ (Fig. 2E) also demonstrates localization with high intensity at all adipocytes in the imaging field, indicating that all adipocytes have incorporated D_{31}-PA. The between-adipocyte differences in D_{31}-PA incorporation are further investigated below. We also find that the $\upsilon_{as}(C\text{-}D)_{2+3}$ signal is located at reduced intensity within the surrounding stroma cells.

In Fig. 2F, we demonstrate how FTIR technology can be applied to determine the subcellular deposits of highly concentrated D_{31}-PA, among other lipids, in a single adipocyte. Figure 2Fi shows a high-magnification FTIR image of adipocyte 1 (indicated in the corresponding optical image in Fig. 2A) using the lipid ester υ_s(C=O):amide I intensity distribution, because it provides good contrast

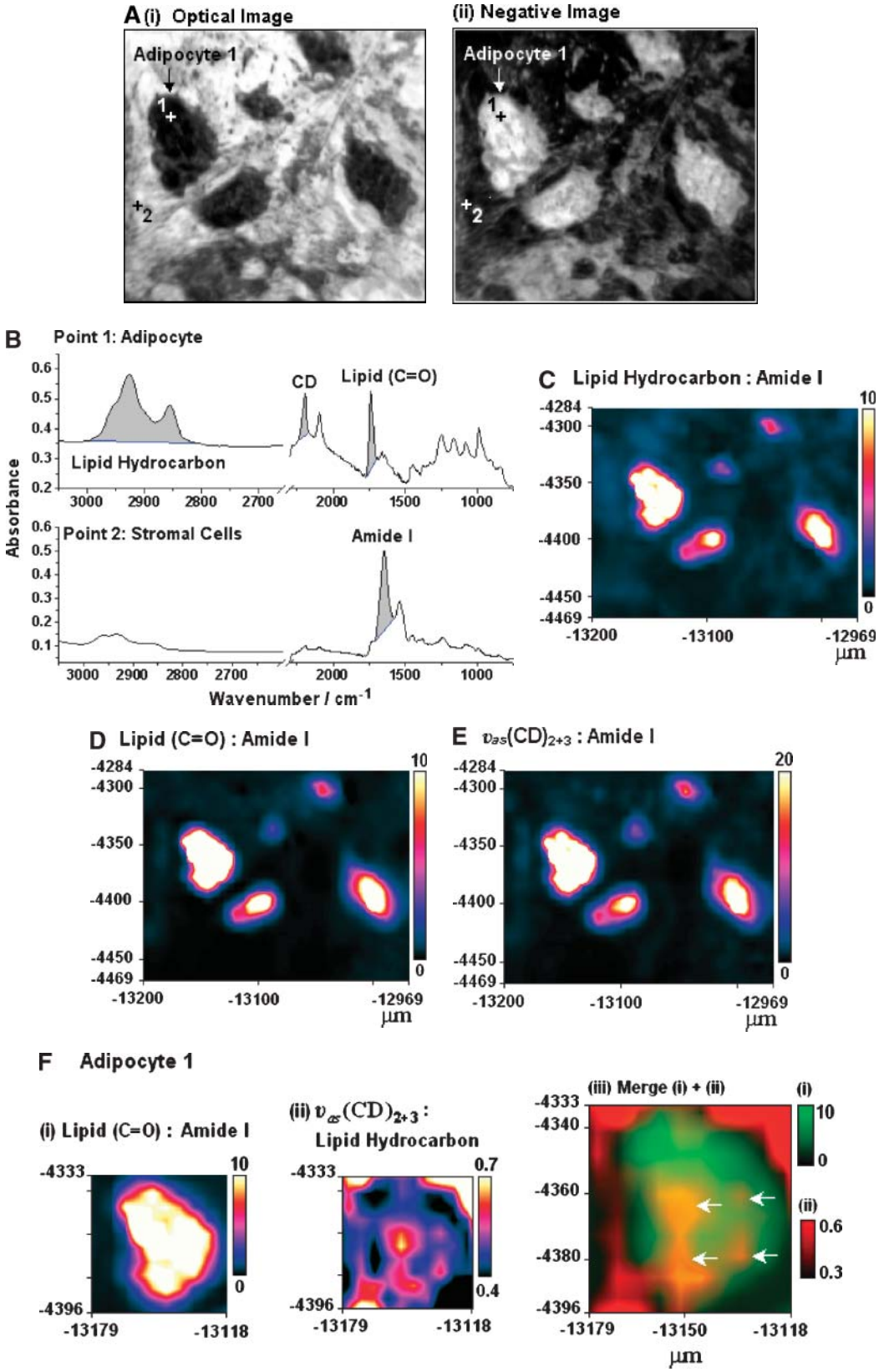

Fig. 2. Localization of concentrated D_{31}-PA in a single adipocyte. A: Optical photomicrograph showing PF-OsO_4-CPD-fixed adipocytes loaded with D_{31}-PA (i). Negative of (i) for better visualization of lipid droplets within the fixed adipocytes (ii). The white arrows identify areas of high $\upsilon_{as}(CD)_{2+3}$ signal, relative to native lipid hydrocarbon. B: Raw FTIR spectra obtained from point 1 (adipocyte) and point 2 (stromal cells), as shown in photomicrograph in A. The method of baseline integration (blue line) and peak areas (gray) used to generate images C–F is shown. FTIR maps of adipocytes depicting the intensity distributions of the lipid hydrocarbon:amide I (C), lipid υ_s(C=O): amide I (D), and $\upsilon_{as}(CD)_{2+3}$:amide I (E) signals. F: Zoomed lipid υ_s(C=O):amide I image of adipocyte 1 (i, red channel); $\upsilon_{as}(CD)_{2+3}$:lipid hydrocarbon image of adipocyte 1 (ii, green channel); and a merge of zoomed adipocyte 1 images (iii).

between the adipocyte and surrounding stromal cells. Figure 2Fii shows the $\upsilon_{as}(C\text{-}D)_{2+3}$:lipid hydrocarbon signal distribution for adipocyte 1 and is used to identify regions of the most highly concentrated D_{31}-PA relative to non-isotopically labeled lipids. For this, the $\upsilon_{as}(C\text{-}D)_{2+3}$ signal was ratioed against the lipid hydrocarbon signal in preference to the lipid ester $\upsilon_s(C{=}O)$ signal, because the latter originates from both nonisotopically labeled lipids and D_{31}-PA. A merge of Fig. 2Fi (color coded with red channel) and Fig. 2Fii (color coded with green channel) gives rise to Fig. 2Fiii, which shows the subcellular localizations of highly concentrated D_{31}-PA molecules (yellow pixels), designated by white arrows.

We further investigated the lipid composition within adipocyte 1 by determining the subcellular locations of the most-concentrated TAG store. As mentioned earlier, although the frequency of absorption for the lipid $\upsilon_s(C{=}O)$ of FFA and TAG overlap, the peak maxima occur at well-separated wavenumbers. The peak maximum for TAG arises at 1,741 cm^{-1}, whereas the lipid $\upsilon(C = O)$ peak maximum for the FFA standard absorbs at 1,714 cm^{-1} (21). However, these wavenumber values may shift in biological samples, depending on the bonding environment of the lipid $\upsilon_s(C{=}O)$ moiety. Gomez-Fernandez et al. (19) report that the protonated carboxyl (COOH) group of FFAs appears at ~1,725 cm^{-1}, and Chalmers (20) has assigned a wave number range of 1,690–1,710 cm^{-1}. We use the upper limit of absorption for the lipid $\upsilon_s(C{=}O)$ moiety as 1,725 cm^{-1}, because one can observe in our spectra, reported in **Fig. 3A**, a shoulder on the lipid $\upsilon_s(C{=}O)$ peak at this wave number due to the FFA, which also conforms to Gomez-Fernandez et al. (18). In addition, we have previously shown that the intensity of absorption of wavenumbers below 1,725 cm^{-1} increases as the relative ratio of FFA to glycerol-bound lipids increases (21).

Figure 3Ai shows the FFA:TAG intensity image for the entire area shown in the optical image in Fig. 2A. This was generated by the ratio of peak areas 1,725–1,699 cm^{-1} (FFA):1,725–1,771 cm^{-1} (glycerol-bound FA, TAG) following baseline integration between 1,771 and 1,699 cm^{-1} (Fig. 3Aii). The intensity image in Fig. 3Ai demonstrates a lower TAG signal at the periphery of the larger adipocytes, which gradually increases toward the interior of each adipocyte, where the majority of TAG is located.

Adipocyte 1, shown in Fig. 3Ai, was magnified and presented in Fig. 3Bi. Figure 3Bii shows baseline corrected FTIR spectra for the lipid $\upsilon_s(C{=}O)$ spectral region, extracted from three different locations in adipocyte 1 (marked 1–3 in Fig. 3Bi). These spectra show that there is an increase in absorption from TAG at >1,725 cm^{-1}, between the spectrum collected at the cell periphery and spectra collected at internal locations. Accompanying this, there is an increase in cell thickness between the cell periphery and location 3, as depicted by the lipid intensity image (inset in Fig. 3Bi). This confirms that the storage of TAG molecules in the adipocyte is the dominating factor influencing its volume. In contrast to the intracellular TAG concentration, there appears to be little change in the FFA absorption at <1,725 cm^{-1}, between spectra collected at the periphery (location 1) of the adipocyte and those collected at internal locations (locations 2 and 3). Edens et al. (22) report that in adipose tissue, stored TAG

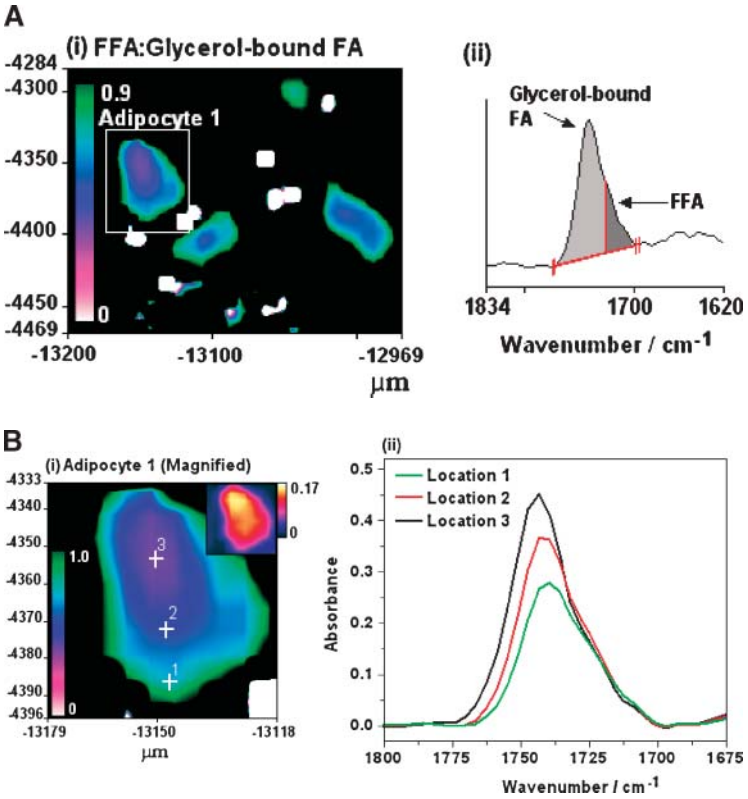

Fig. 3. Distributions of TAG and FFAs in a single adipocyte. A: Free FA (FFA):glycerol-bound FA (TAG) intensity image (i); Raw FTIR spectrum with baseline integration and peak areas (dark and light gray) used to define the amounts of glycerol-bound FA and FFA (ii). These peak areas were ratioed to produce the intensity image in i. B: Magnified FFA:glycerol-bound FA intensity image of adipocyte 1 (identified by white box in A) (i). The inset shows a lipid hydrocarbon intensity image of adipocyte 1, depicting changes in the thickness of adipocyte 1; FTIR spectra were acquired from a region of high FFA:glycerol-bound FA signal at the periphery of the adipocyte (location 1), an intermediate signal (location 2) and a low signal (location 3) (ii).

undergoes continuous, simultaneous synthesis and breakdown. The data reported here (Fig. 3) suggest that within a single adipocyte, the FFAs are broken down or are in the process of being synthesized into TAG around an internalized TAG store.

We next studied the amount of D_{31}-PA incorporation, relative to other FAs from the adipogenic media, between adipocytes, and its association with cell size. SR-FTIR spectra were obtained from 20 different PF-OsO_4-CPD adipocytes that varied in size. The baseline corrected lipid hydrocarbon $\upsilon_{as+s}(\text{C-H})_{2+3}$ peak area was used to represent the amount of FAs other than the isotopically labeled D_{31}-PA, which was represented by the intensity of the $\upsilon_{as+s}(\text{C-D})_{2+3}$ peak area (**Fig. 4A**). Note that the cross sections of the $\upsilon_{as+s}(\text{C-H})_{2+3}$ and $\upsilon_{as+s}(\text{C-D})_{2+3}$ signals are different, with the $\upsilon_{as+s}(\text{C-D})_{2+3}$ signal being lower. For an isolated C-D bond, the intensity would be $1 / \sqrt{2}$ lower than the equivalent C-H signal. However, for multiple bonds in a larger molecule, this relationship is complicated by neighboring molecules and difficult to determine. We have therefore simply used the band intensities uncorrected for cross section differences to provide a lower limit of the percent D_{31}-PA. Figure 4B shows the association of percent D_{31}-PA [$\upsilon_{as+s}(\text{C-D})_{2+3}$ / [($\upsilon_{as+s}(\text{C-H})_{2+3}$ + $\upsilon_{as+s}(\text{C-D})_{2+3}$)] of the total adipocyte lipids, incorporated into the adipocyte, with adipocyte size. A noticeable trend in the data presented in Fig. 4B is that there are no adipocytes with sizes greater than ~7,000 μm^2 that give rise to percent D_{31}-PA values of less than 25%, whereas the inverse is true for adipocytes with sizes less than ~7,000 μm^2. Thus, these data suggest a general trend in which larger adipocytes contain higher concentrations of percent D_{31}-PA, up to a limiting concentration of 30–35%.

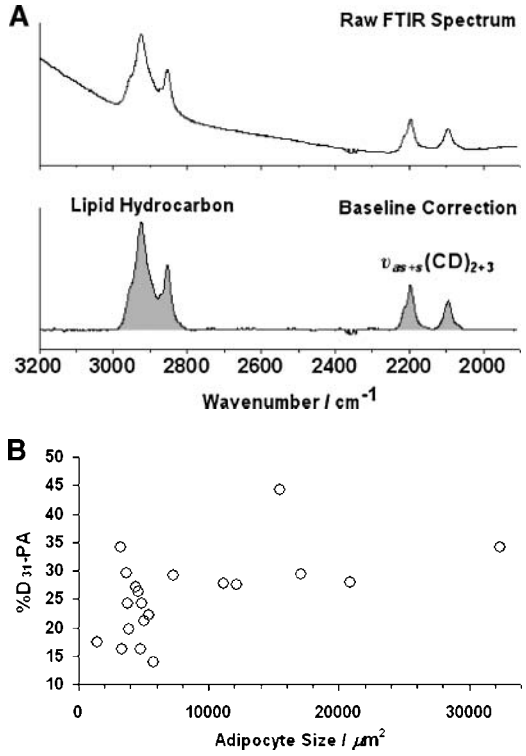

Fig. 4. The relationship between percent D_{31}-PA incorporated into adipocytes and adipocyte size. A: An example of baseline correction of a raw FTIR spectrum in the frequency range 3,200–1,900 cm^{-1} collected from adipocyte lipid droplets. The $\upsilon_{as+s}(CD)_{2+3}$ and the lipid hydrocarbon peak areas were used to calculate percent D_{31}-PA of total lipids in the adipocyte; B: Scatterplot showing the relationship between percent D_{31}-PA in adipocytes and adipocyte size (μm^2), derived from FTIR spectra of 20 adipocytes.

Tracking the translocation of D_{31}-PA from adipocytes into PC-3 cells

Serum-starved PC-3 cells were incubated with D_{31}-PA-loaded adipocytes for 48 h prior to fixation. **Figure 5A** shows an optical image of a PF-OsO_4-CPD-fixed adipocyte surrounded by PC-3 cells and stroma cells. In this figure, the adipocytes are visualized as large dark bodies (designated Adp. in Fig. 5Ai), whereas PC-3 cells (1–4 in Fig. 5Aii) are lighter in appearance and possess lamellipodia/pointed processes. The boxed area was mapped using FTIR microspectroscopy, and the $\upsilon_{as}(\text{C-D})_{2+3}$ signal intensity distribution is shown in Fig. 5B. As expected, we observe localization of the $\upsilon_{as}(\text{C-D})_{2+3}$ signal with high intensity at the adipocyte; however, we also find that this signal illuminates the PC-3 cells (Fig. 5B). Because the only source of $\upsilon_{as}(\text{C-D})_{2+3}$ signal in the PC-3 cells is D_{31}-PA released by the adipocytes, these data suggest translocation of D_{31}-PA from the adipocytes into the PC-3 cells.

It is possible that the $\upsilon_{as}(\text{C-D})_{2+3}$ signal in the PC-3 cells is due to background $\upsilon_{as}(\text{C-D})_{2+3}$ absorption from stroma cells that may reside beneath the PC-3 cells. Baseline corrected FTIR spectra, in the frequency range comprising C-D absorbencies, were extracted from PC-3 cells (1–4) and extracellular locations (Sub 1–3) in close proximity to the PC-3 cells (Fig. 5C). The integrated areas of the C-D peaks are also displayed for these spectra in Fig. 5C. In Fig. 5Aii, we observe that the extracellular substrate adjacent to PC-3 cells 3 and 4 is optically absent of stroma cells. A spectrum was taken from this background location, as shown in Fig. 5B, and presented in Fig. 5C, Sub 1. This raw spectrum of the substrate reveals that the C-D peaks cannot be resolved from spectral noise (Fig. 5C). However, the spectrum of PC-3 cells 3 and 4 (Fig. 5C), which is in close proximity to this blank substrate (see optical image in Fig. 5A), gives rise to two prominent C-D peaks, demonstrating the translocation of D_{31}-PA from the adipocyte into the PC-3 cell. A similar case is also found for PC-3 cell 1 (Fig. 5C), which displays two C-D peaks that are well resolved from spectral noise and whose adjacent background spectrum (Sub 3) displays no significant C-D absorbencies that can be resolved from spectral noise. For PC-3 cell 2, we find that this cell resides on a substrate/stroma cell background that gives rise to C-D peaks with appreciable absorbencies of 0.33 and 0.17 cm^{-1} (Fig. 5C). Nevertheless, even after subtraction of this background, the C-D peak areas in the spectrum of PC-3 cell 2 provide values of 0.64 and 0.33 cm^{-1}.

It is interesting to note that the intensity of C-D signal from the PC-3 cells is in the order of PC-3 cell 4 < cell 3

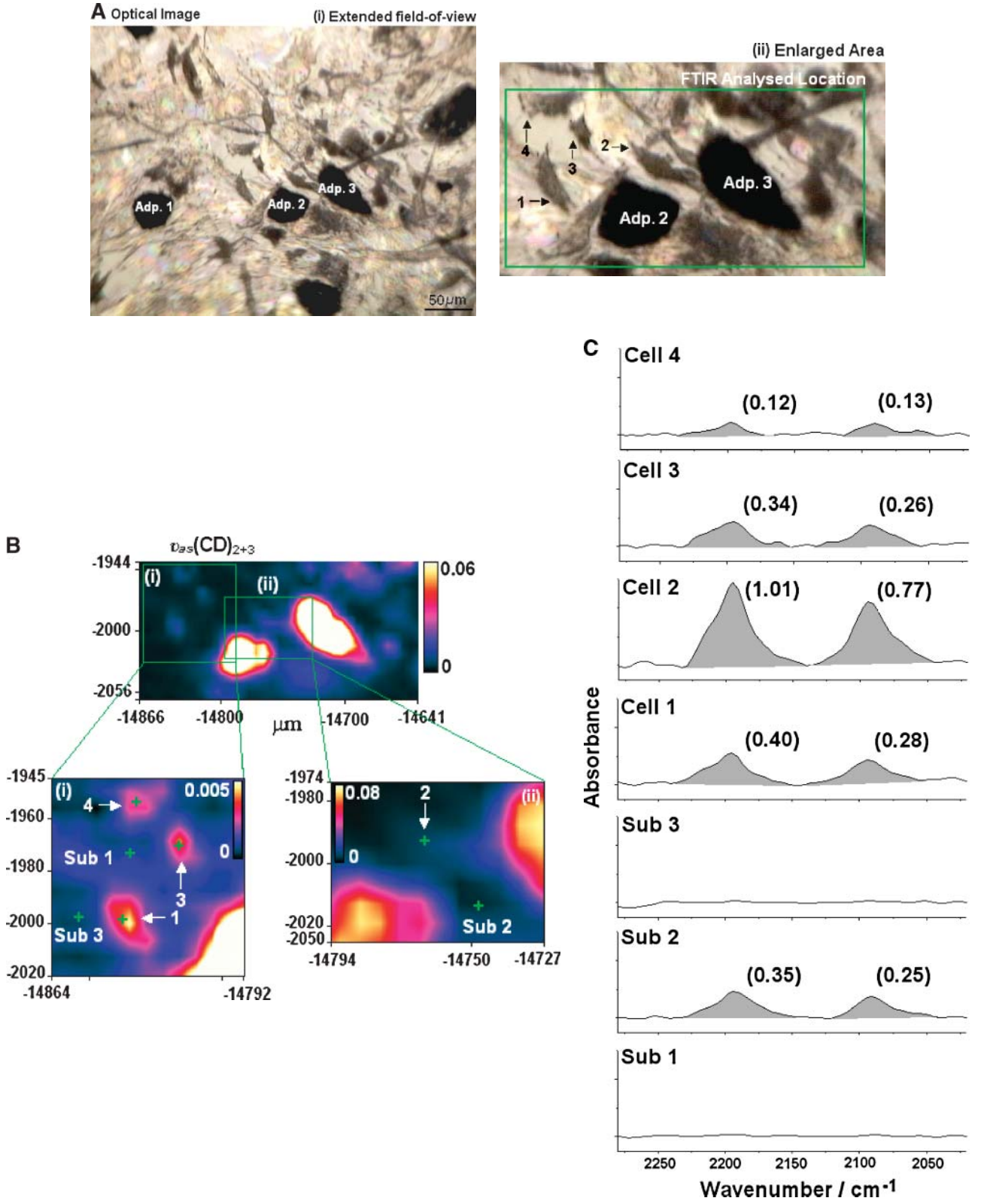

Fig. 5. D_{31}-PA translocation between adipocytes and PC-3 cells. A: Optical photomicrograph showing PF-OsO_4-CPD adipocytes (Adp. 1–3) surrounded by PC-3 cells and stroma cells (i); magnified region of Adp. 2 and 3 with surrounding PC-3 cells (labeled 1–4) (ii). The boxed area was analyzed by imaging FTIR microspectroscopy. B: FTIR spectral maps depicting the intensity distribution of the $\upsilon_{as}(CD)_{2+3}$ signal. The boxed areas (i) and (ii) were expanded and the color intensity threshold changed to provide better contrast of the $\upsilon_{as}(CD)_{2+3}$ signal in cells relative to the substrate. C: Baseline corrected FTIR spectra taken from PC-3 cells 1–4 and adjacent extracellular substrate/stem cells (Sub 1–3) locations are presented for the C-D spectral region. The integrated peak areas for the C-D peaks are shown in parentheses. The absorbance scale for each spectrum is identical, with upper and lower limits set as 0 and 0.03, respectively.

and cell 1 < cell 2, which correlates with their distances from the adipocytes (Fig. 5A).

DISCUSSION

The deposition and metabolism of FAs in adipocytes, along with the cellular environment of adipose tissue at different sites in the body, can vary significantly (23–25). These anatomical-specific variations in adipose tissue biochemistry could influence the FA content of adipocytes. In addition, it has not been confirmed whether there is a genetic basis for the requirement for an adipocyte to incorporate specific FAs and whether this predisposition, if present, is different between body sites. Therefore, to study the interaction of metastatic bone marrow-derived PC-3 cells with adipocytes, we used isolated MSCs from primary bone marrow tissue and differentiated these into the adipocyte lineage.

Prior to investigations concerning the uptake of FAs from adipocytes into PC-3 cells, issues concerning sample preparation were addressed. This was found to be a necessity, because delocalization/bleeding of lipid molecules from adipocytes in our adipocyte-PC-3 cell coculture system could arise in false-positive results concerning PC-3 uptake of adipocyte-derived D_{31}-PA. Moreover, we found that in the absence of chemical fixation, the structured intracellular lipid droplets would collapse into a lipid deposit (Fig. 1B), and many adipocytes would lose a large number of lipid molecules (readily observed through optical microscopy), perhaps through air-oxidation of volatile unsaturated FAs. Fixation preserves not only the morphological information but also the spatial localization of the subcellular biomolecules of the adipocyte-PC-3 cell coculture system. Chemical fixation was chosen in preference to flash freezing and freeze drying for reasons outlined previously by our group (18).

The use of OsO_4 as a postfixative for preserving the localization of lipid droplets in adipocytes is well documented (26–28). However, a disadvantage of OsO_4 fixation is that the OsO_3 by-product following OsO_4 reaction with the lipid (Fig. 1E) can dissociate to form OsO_2, which is a black, insoluble precipitate (29). Unbound OsO_3 should be washed away during the Sorensen's buffer washing step and dehydration steps before CPD. However, even following these extensive washing steps, we obtain some darkening of the adipocytes as a result of OsO_2 precipitation, as observed for the adipocytes in Figs. 2A and 5A. Although the amount of OsO_2 precipitate is different between these adipocytes, this does not influence our FTIR analysis, because OsO_2 does not absorb IR light in the mid-IR spectral region.

Following our assessment of adipocyte fixation, we evaluated, for the first time, the molecular information that could be derived from the adipocyte through FTIR microspectroscopy. As expected, high lipid hydrocarbon and lipid ester υ_s(C = O) signals (Fig. 2C, D, respectively) were measured from the adipocytes, compared with the stroma cells, and an increase in contrast was observed between adipocytes and stroma cells using the lipid ester υ_s(C=O) signal. Together, these results highlight that a high proportion of the adipocyte volume is lipid; in fact, Frühbeck et al. (15) have reported it to be ~90%. The high contrast observed between adipocytes and stroma cells, using the lipid ester υ_s(C = O) intensity distribution, arises because most of the adipocyte lipid is in the form of a concentrated store of TAG, with each TAG comprising three fatty acyl chains bonded via an ester moiety to a glycerol backbone.

The identification of intracellular D_{31}-PA hot spots in the FTIR image of adipocyte 1 through the intensity distribution of $\upsilon_{as}(\text{C-D})_{2+3}$:lipid hydrocarbon signal (Fig. 2Fiii) may have significance in relation to adipocyte metabolism. Free FA (FFA) reesterification in adipocytes refers to the cycle of TAG hydrolysis for FFA liberation, its release from the adipocyte into the extracellular environment, and then reabsorption into the adipocyte for reesterification and TAG synthesis (22). Edens, Leibel, and Hirsch (22) have reported that this loop requires functionalized compartmentalization of FFA within the adipocyte, which prevents access of lipolytically derived FFA to the enzymes of glycerolipid synthesis. Thus, the hot spots of high $\upsilon_{as}(\text{C-D})_{2+3}$ signal could correspond to TAG as well as FFA-compartmentalized D_{31}-PA in adipocyte 1 (Fig. 2Fiii). In fact, the FFA:TAG image in Fig. 3B for adipocyte 1 can provide information concerning the molecular state of these D_{31}-PA-rich locations. The D_{31}-PA hot spots in Fig. 2Fiii overlapping with the TAG-rich locations in Fig. 3Bi may correspond to D_{31}-PA as TAG, whereas the D_{31}-PA hot spots overlapping with FFA-rich locations may correspond to D_{31}-PA in the form of FFAs. However, further processing of other adipocytes analyzed by FTIR microspectroscopy (data not shown) revealed that these discrete subcellular locations of highly concentrated D_{31}-PA were not observed for all adipocytes.

The localization of an isotopically labeled FA in a single adipocyte was also studied by Kleinfeld, Kampf, and Lechene (30) through multi-imaging mass spectrometry (MIMS). However, the adipocytes used in that study (30) were removed from media and dried under argon, which may have negative effects on the subcellular localization and structural integrity of the delicate lipid droplets. Although relative quantifications of a labeled FA within the adipocyte cytosol and lipid droplets were approximated using partition coefficients, it is unclear from their work (30) how this information was obtained, because direct MIMS analysis of the adipocyte interior must be accessed through freeze fracture or depth profiling. In contrast, FTIR microspectroscopy is less invasive, because it does not require fracture to access intracellular information and fixation can be applied to preserve the structural and spatial integrity of the lipid droplets. Another system that can be used to image the incorporation of specific lipids into the droplets of adipocytes is polyene tagging of lipids with two-photon excitation fluorescence microscopy (31). Compared with FTIR microspectroscopy, this system can provide better spatial resolution for localizing tagged

lipids to subcellular compartments; however, saturated lipids such as palmitic acid cannot be studied using the fluorescence technique.

The quantitative study of specific FA uptake into an adipocyte and its influence on cell size is of particular interest in oncology because it has been reported that the concentration of unsaturated FAs in adipose tissue in breast cancer patients was in negative correlation with adipocyte size, whereas this correlation was reversed in lung cancer patients (24). In the present in vitro study, a scatterplot (Fig. 4B) indicated that the larger bone marrow-derived adipocytes stored a greater amount of D_{31}-PA relative to nonisotopically labeled FAs. The data presented in Fig. 4B demonstrate that the uptake of a specific FA as a function of adipocyte size can be carried out without lipid extraction or adipocyte isolation and size exclusion from whole single adipocytes, in vitro, using FTIR microspectroscopy. In the context of adipocyte-tumor cell associations, the FTIR methodology reported here can be used to correlate the percentage of incorporation of a specific FA by the adipocyte with its size when these adipocytes are cocultured with and without tumor cells.

However, a limitation of this technique is associated with FA chain modification as a result of desaturase activity. If a significant amount of incorporated D_{31}-PA is desaturated and stored as TAG in the adipocytes, then this situation would cause a reduction in the $\upsilon_{as+s}(C\text{-}D)_2$ signal. Chain elongation will not affect the correlation between the amount of D_{31}-PA incorporated into the adipocyte and its size, because the number of $C\text{-}D_2$ moieties will remain the same.

The final part of our work studied the translocation of D_{31}-PA from adipocytes into PC-3 cells. To date, there are only a few publications in the current literature that report on an upregulation of lipids in tumor cells in the presence of adipocytes (9, 13). However, one cannot assume, without lipid-tracing experiments, that the observed upregulation of these cytoplasmic lipid droplets in the tumor cell is due to lipid translocation from adipocytes into the tumor cell. This is because tumor cells are known to upregulate lipid biosynthesis de novo through the overexpression of lipogenic enzymes, which have been reported to be induced by growth factors and hormones (32, 33). It is known that adipocytes release a range of growth factors (15), and these may stimulate the tumor cell to express lipogenic enzymes for de novo lipid biosynthesis. The data presented in Fig. 5 provide the first direct experimental evidence that the upregulation of lipid droplets in PC-3 cells, when cocultured with adipocytes, is at least in part due to FA translocation between the adipocyte and the PC-3 cell.

Although the translocation of D_{31}-PA from the adipocyte into the PC-3 cell has been unequivocally demonstrated in this study using isotopically labeled D_{31}-PA as a tracer, it is not known whether this translocation is mediated through direct PC-3 cell-adipocyte contact or via uptake from the incubation medium following FFA release from the adipocyte. In light of the data presented here, the high C-D signal from PC-3 cell 2, which resides between two adipocytes (Adp. 2 and 3, Fig. 5Aii), may have capitalized on both processes for D_{31}-PA uptake; whereas PC-3 cell 4, at 88 μm from adipocyte 1 and 75 μm from adipocyte 3, furthest away from all of the adipocytes within the field of view, may have only incorporated released D_{31}-PA from the media, giving rise to a lower C-D signal than cell 2. These hypotheses are currently being investigated in our laboratory.

The in vitro system described here provides a foundation for further investigations aimed at determining the specific FAs that may be incorporated/preferred by tumor cells (as well as associated mechanisms of uptake) and their biological consequences. In a wider context, this molecular-based assay can complement and provide support for epidermiological findings correlating dietary fat with cancer risks; Dennis et al. (5) have highlighted inconsistencies in these studies with respect to measurement differences for estimating service sizes (definitions of food groups or instructions provided to responders) and reporting methods (questionnaire platforms).

CONCLUSION

In summary, we have shown the importance of chemical fixation for studying adipocytes by FTIR microspectroscopy in terms of lipid droplet preservation. Using human bone marrow-derived D_{31}-PA-loaded adipocytes, we demonstrated for a single adipocyte the subcellular locations enriched with D_{31}-PA as well as its TAG:FFA intensity profile. We found that larger adipocytes incorporate higher amounts of D_{31}-PA, which demonstrates the feasibility of FTIR microspectroscopy for studying the association of a specific FA with adipocyte size in whole adipocytes. Most importantly, this study categorically demonstrates that lipid translocation takes place between PC-3 cells and human-derived adipocytes.

We acknowledge the Association for International Cancer Research for financial support (E.G.). We thank Dr. Fariba Bahrami and Dr. James Nicholson (Daresbury Laboratory, UK) for help during SR-FTIR microspectroscopy measurements and for the use of the Spotlight FTIR instrument. We also thank Dr. Stephen Murray (Paterson Institute, UK) for help during adipocyte fixation.

REFERENCES

1. Cancer Research UK. 2006. UK prostate cancer incidence statistics. Accessed February 21, 2007 at http://info.cancerresearchuk.org/cancerstats/types/prostate/incidence/.
2. Cancer Research UK. 2007. UK cancer mortality statistics for males. Accessed February 21, 2007 at http://info.cancerresearchuk.org/cancerstats/mortality/males/?a=5441.
3. Giovannucci, E., E. B. Rimm, G. A. Colditz, M. J. Stampfer, A. Ascherio, C. C. Chute, and W. C. Willett. 1994. A prospective study of dietary fat and risk of prostate cancer. *J. Nat. Cancer Inst.* **86:** 1571–1579.
4. Nomura, A. M., and L. N. Kolonel. 1991. Prostate cancer: a current perspective. *Epidemiol. Rev.* **13:** 200–227.
5. Dennis, L. K., L. G. Snetselaar, B. J. Smith, R. E. Stewart, and

M. E. C. Robbins. 2004. Problems with the assessment of dietary fat in prostate cancer studies. *Am. J. Epidemiol.* **160:** 436–444.
6. Rodriguez, C., A. V. Patel, E. E. Calle, E. J. Jacobs, A. Chao, and M. J. Thun. 2001. Body mass index, height, and prostate cancer mortality in two large cohorts of adult men in the United States. *Cancer Epidemiol. Biomarkers Rev.* **10:** 345–353.
7. Amling, C. L., C. K. Kane, R. H. Riffenburgh, J. F. Ward, J. L. Roberts, R. S. Lance, P. A. Friedrichs, and J. W. Moul. 2001. Relationship between obesity and race in predicting adverse pathologic variables in patients undergoing radical prostatectomy. *Urology.* **58:** 723–728.
8. Salazar, O. M., P. Rubin, and F. R. Hendrickson, Komaki R., Poulter C. Newall, J. Asbell, S. O., Mohiuddin, M., and Van Ess, J. 1986. Single-dose half-body irradiation for palliation of multiple bone metastases from solid tumors. Final Radiation Therapy Oncology Group report. *Cancer.* **58:** 29–36.
9. Brown, M. D., C. A. Hart, E. Gazi, S. Bagley, and N. W. Clarke. 2006. Promotion of prostatic metastatic migration towards human bone marrow stroma by omega 6 and its inhibition by omega 3 PUFAs. *Br. J. Cancer.* **94:** 842–853.
10. Ookhtens, M., D. Montisano, I. Lyon, and N. Baker. 1997. Transport and metabolism of extracellular free fatty acids in adipose tissue of fed and fasted mice. *J. Lipid Res.* **28:** 528–539.
11. Sethi, J. K., and G. S. Hotamisligril. 1999. The role of TNFα in adipocyte metabolism. *Cell Dev. Bio.* **10:** 19–29.
12. Kopelman, P. G. 1998. Effects of obesity on fat topography: metabolic and endocrine determinants. *In* Clinical Obesity. 1st edition. P. G. Kopelman and M. J. Stock, editors. Blackwell Science, Oxford, UK. 158–175.
13. Tokuda, Y., Y. Satoh, C. Fujiyama, S. Toda, H. Sugihara, and Z. Masaki. 2003. Prostate cancer cell growth is modulated by adipocyte-cancer cell interaction. *BJU Int.* **91:** 716–720.
14. Onuma, M., J. D. Bud, T. L. Rummel, and Y. Iwamoto. 2003. Prostate cancer cell –adipocyte interaction. *J. Biochem. (Tokyo).* **278:** 42660–42667.
15. Frühbeck, G., J. Gomez-Ambrosi, F. J. Muruzabal, and M. A. Burrell. 2001. The adipocyte: a model for integration of endocrine and metabolic signaling in energy metabolism regulation. *Am. J. Physiol. Endocrinol. Metab.* **280:** E827–E847.
16. Metzger, S., T. Hassin, V. Barash, O. Pappo, and T. Chajek-Shaul. 2001. Reduced body fat and increased hepatic lipid synthesis in mice bearing interlukin-6-secreting tumor. *Am. J. Physiol. Endocrinol. Metab.* **281:** E957–E965.
17. StemCell Technologies. 2004. RosetteSep™ Mesenchymal Stem Cell Enrichment Cocktail. Procedure and product information. Accessed April 19, 2007 at https://www.stemcell.com/technical/15128_15168-PIS.pdf.
18. Gazi, E., J. Dwyer, N. P. Lockyer, P. Gardner, J. Miyan, C. A. Hart, M. D. Brown, and N. W. Clarke. 2005. Fixation protocols for subcellular imaging by synchrotron-based Fourier transform infrared microspectroscopy. *Biopolymers.* **77:** 18–30.
19. Gomez-Fernandez, J. C., and J. Villalain. 1998. The use of FT-IR for quantitative studies of the apparent pKa of lipid carboxyl groups and the dehydration degree of the phosphate group of phospholipids. *Chem. Phys. Lipids.* **96:** 41–52.
20. Chalmers, J. M. 2002. Spectra-structure correlations in the mid- and far-infrared. *In* Handbook of Vibrational Spectroscopy. Vol. 3. J. M. P. Chalmers and, R. Griffiths, editors. John Wiley and Sons, Chichester, U.K. 1790–1816.
21. Gazi, E., J. Dwyer, N. P. Lockyer, P. Gardner, J. H. Shanks, J. Roulson, C. A. Hart, N. W. Clarke, and M. D. Brown. 2007. Biomolecular profiling of metastatic prostate cancer cells in bone marrow tissue using FTIR microspectroscopy: a pilot study. *Anal. Bioanal. Chem.* **387:** 1621–1631.
22. Edens, N. K., R. L. Leibel, and J. Hirsch. 1990. Mechanism of free fatty acid re-esterification in human adipocytes in vitro. *J. Lipid Res.* **31:** 1423–1481.
23. Romanski, S. A., R. M. Nelson, and M. D. Jensen. 2000. Meal fatty acid uptake in human adipose tissue: technical and experimental design issues. *Am. J. Physiol. Endocrinol. Metab.* **279:** E447–E454.
24. Arner, P. 1984. Site differences in human subcutaneous adipose tissue metabolism in obesity. *Aeth. Plast. Surg.* **8:** 13–17.
25. Rink, J. D., E. R. Simpson, J. J. Barnard, and S. E. Bulun. 1996. Cellular characterization of adipose tissue from various body sites of women. *J. Clin. Endocrinol. Metab.* **81:** 2443–2447.
26. Richardson, R. L., G. J. Hausman, D. R. Campion, and G. B. Thomas. 1986. Adipocyte development in primary rat cell cultures: a scanning electron microscopy study. *Anat. Rec.* **216:** 416–422.
27. Julien, P., J. P. Despres, and A. Angel. 1989. Scanning electron microscopy of very small fat cells and mature fat cells in human obesity. *J. Lipid Res.* **30:** 293–299.
28. Eguinoa, P., S. Brocklehurst, A. Arana, J. A. Mendizabal, R. G. Vernon, and A. Purroy. 2003. Lipogenic enzyme activities in different adipose depots of Pirenaican and Holstein bulls and heifers taking into account adipocyte size. *J. Anim. Sci.* **81:** 432–440.
29. Kieran, J. A. 1990. Histological and Histochemical Methods: Theory & Practice. Pergamon Press, Oxford, UK. 12–27.
30. Kleinfeld, A. M., J. P. Kampf, and C. Lechene. 2004. Transport of ^{13}C-oleate in adipocytes measured using multi imaging mass spectrometry. *J. Am. Soc. Mass Spectrom.* **15:** 1572–1580.
31. Kuerschner, L., C. S. Ejsing, K. Ekroos, A. Shevchenko, K. I. Anderson, and C. Thiele. 2005. Polyene-lipids: a new tool to image lipids. *Nat. Methods.* **2:** 39–45.
32. Swinnen, J. V., K. Brusselmans, and G. Verhoeven. 2006. Increased lipogenesis in cancer cells: new players, novel targets. *Curr. Opin. Clin. Nutr. Metab. Care.* **6:** 358–365.
33. Hannelore, H., B. Maes, F. Foufelle, W. Heyns, G. Verhoeven, and V. J. Swinnen. 2001. Androgens stimulate lipogenic gene expression in prostate cancer cells by activation of the sterol regulatory element-binding protein cleavage activating protein/sterol regulatory element-binding protein pathway. *Mol. Endocrinol.* **15:** 1817–1828.